JOURNAL OF MATERIALS SCIENCE **37** (2002) 3415–3421

Temperature and branching dependence of surface extrusion instabilities in metallocene catalysed polyethylene

M. AGUILAR, J. F. VEGA
GIDEM, Instituto de Estructura de la Materia, CSIC, Serrano 113-123, 28006 Madrid, Spain

A. MUÑOZ-ESCALONA
Repsol I+D, Embajadores 183, 28045 Madrid, Spain

J. MARTÍNEZ-SALAZAR*
GIDEM, Instituto de Estructura de la Materia, CSIC, Serrano 113-123, 28006 Madrid, Spain
E-mail: jmsalazar@iem.cfmac.CSIC.es

We have found a branching dependence of critical extrusion temperature in metallocene-catalysed linear and branched polyethylene, below which the commonly found surface distortion instabilities disappear. The elimination of these extrusion instabilities has been observed in a wide range of temperatures up to 23°C above the melting point of each polymer. However, in contrast to previous observations, a window of minimum flow resistance, i.e., extrusion pressure, is not detected. This low temperature effect is discussed in terms of a flow ordered phase at the wall that induces local chain orientation. This so-called mesophase would prevent the mechanism for the formation of distortions to operate below a critical temperature.

1. Introduction

Conventional processing and melt testing in polyethylene (PE) are usually performed at temperatures above 160°C. In these conditions the material is completely molten and the viscous flow is reduced in such a way that an easy transformation can be carried out. However, for high molecular weight (M_w) polymers with a narrow molecular weight distribution (MWD), flow instabilities and extrudate distortions become important effects in standard operation conditions. In this case, processing aids [1, 2] and/or specially designed orifices (different kinds of material of construction [3], fluorinated surfaces [4] and porous media at the entrance of the orifice [5]) have to be used in order to eliminate or at least minimise the irregularities.

However, despite the great effort invested on this fundamental research topic, the origin of the extrudate distortions is still a controversial issue [6]. It was initially established that distortions were the result of a crack formation mechanism due to the action of high tensile stresses that presumably developed at the exit-die region [7, 8]. Following this approach Cogswell found in a systematic study that the surface layer of the melt near the wall broke above a certain critical value of the extrudate velocity [9]. More recent works by El Kissi *et al*. [10] as well as numerical simulations by Mackley *et al*. [11] still support this idea. A completely different view links the appearance of these defects with wall slip at the polymer-wall interface [3, 12, 13]. For this latter case some models have been developed to take into account the chain stretching during the detachment process from the wall [14, 15]. A more recent approach by Brochard and de Gennes [16] considers a coil-stretch transition of grafted chains from the bulk, i.e., a disentanglement mechanism, as the main cause of the slip phenomena. On the other hand, Wang *et al*. [17, 18] have postulated the existence of a double mechanism: chain disentanglement and adhesive failure for weakly adsorbed species from the capillary wall. Some efforts have been made to integrate the different mechanisms in an unified network model able to predict both the appearance of flow distortions and the wall slip phenomenon either by a disentanglement mechanism or by a debonding mechanism. In both cases the mechanism would be dependent upon the relative adhesive energy of the polymer-wall pair [19], and had to take into account the stretching of the attached molecules [20].

In the past decade an interesting finding by Keller and co-workers [21–26] demonstrated that polymers that are usually difficult to process could be extruded in certain conditions of temperature and shear. In these conditions a sharp increase in fluidity and a parallel disappearance of distortions would take place. In fact a temperature window from 149 to 153°C, depending on molecular weight and shear rate, was reported. The authors claimed the formation of a mobile

*Author to whom all correspondence should be addressed.

hexagonal phase of low viscosity arising through the flow-induced alignment of presumably adsorbed chains at the capillary wall. Assuming the molecular disentanglement/slip model of Wang *et al*. [17, 18] they suggested that, in such an ordered mesophase, the adsorbed chains would remain disentangled and the molecular mechanism causing the distortion would be no longer present. Consequently a continuous slip would take place. Above the critical temperature window (T_{od}), the distortion regimes would appear as a consequence of the destruction of this phase and the onset of chain disentanglement/slip mechanisms.

Unfortunately, the main study of Keller and coworkers [21–26] was carried out using very high molecular weight polydisperse materials. The recent development of metallocene-catalysed polyethylene (*m*-PE) opens up new possibilities to study the effect of molecular parameters in a more systematic way. In fact PE samples with narrow MWD, short chain branching (SCB) with homogeneous distribution and a total absence of long chain branching can be obtained with some catalysts [27]. In the present study a series of metallocene-catalysed ethylene homopolymer and ethylene/1-hexene copolymers have been employed. The molecular weight and polydispersity index of the samples are nearly constant, and the only variable parameter is the degree of comonomer content or number of buthyl branches (from 0 to 11 branches/1000 C atoms). Our interest in this work is primarily focused on how the SCB content in PE affects the low temperature extrusion behaviour of the polymer near and above its melting temperature. However the interpretation of the results requires an analysis of the various surface irregularities that appear during capillary extrusion so other lateral aspects concerning the flow curves will be previously addressed.

2. Experimental

2.1. Materials characterisation

Molecular weight distribution (MWD) was determined by Size Exclusion Gel Permeation Chromatography (SEC) in a 150 CV GPC from Waters and Viscotek Viscometer. Elution of samples was carried out in 1,2,5-trichlorobenzene (TCB) at 145°C . Universal calibration was applied using a set of polystyrene standards. The branch content was determined by ^{13}C-NMR. The ^{13}C-NMR spectra were recorded at 100°C using Brucker AC 300 spectrometer operating at 75 MHz. Sample solution of 20% (v/v) were prepared using deuterated benzene and TCB with trimethylsilane as an internal standard. DSC thermograms have been performed by means of a Perkin-Elmer DSC-7 calorimeter calibrated with Indium in order to obtain the characteristic melt temperature of the crystals (T_m), which, as it is well known, can be correlated with the comonomer content [28]. All these parameters are collected in Table I.

TABLE I Molecular parameters and melting temperature of the materials studied

Material	M_w	M_w/M_n	SCB/1000 C	T_m/°C
WP0	152000	2.3	0	133
WP1	120700	2.2	2.7	126
WP2	116000	2.0	5.5	123
WP3	118200	2.2	10.7	118

2.2. Rheological characterisation

2.2.1. Oscillatory shear measurements

Disk specimens of 25 mm diameter and 1 mm thickness were compression moulded in a Schwabenthan Polystat 200T hot press for 2 minutes at 160°C and a nominal pressure of 150 bars. Rheological measurements were performed in a dynamic thermal analyser Polymer Laboratories torsion rheometer using the parallel plates mode. Oscillatory viscoelastic measurements were carried out covering an angular frequency range between 0.0628 and 628 rad s^{-1}, well inside the linear viscoelastic region. The following viscoelastic functions were measured: storage modulus, $G'(\omega)$; loss modulus, $G''(\omega)$; dynamic viscosity, $\eta^*(\omega)$; and loss tangent, tanδ. The temperature range of measurements was from 130 to 190°C . The time-temperature superposition principle has been applied. Rheological parameters, such as Newtonian viscosity, η_0, and relaxation time, τ_0, have been obtained at a reference temperature of 190°C.

2.2.2. Extrusion measurements

The flow curves of shear stress *versus* shear rate have been obtained in a piston-typs capillary rheometer CEAST Rheoscope 1000. Data have been collected in the shear rate range between 6 and 240 s^{-1} using 1 mm diameter die capillary and a ratio (L/D) of 20. As a first step we have determined for each polymer the critical shear stress values for the onset of the extrudate irregularities, namely the sharskin at σ_{c1} and the slip-stick transition at σ_{c2}. All the experiments have been done at a reference temperature of 160°C. The recognition of each of the irregularities has been performed by visual inspection of the extrudates. In order to monitor the change of the extrudates with temperature we have carried out a set of temperature sweeps at intervals of 2°C. Each temperature run was started at $T_m + 10$°C. We have tested that the stress value is always above σ_{c1} when the piston speed was varied between 2 and 10 mm/s. For each polymer one can define a final temperature T_{od}, indicative of the onset of the irregularities. In order to avoid undesirable crystallisation memory effects we have carried out a second set of measurements after melting the sample above 160°C for a few minutes and then cooling down to the pre-selected temperatures $T_m + 10$°C . Finally the evolution of the distortions has been studied in one of the copolymers keeping constant both the shear stress and the shear rate while varying the temperature.

3. Results and discussion

3.1. Viscoelastic characterisation

Complex viscosity, η^*, *versus* angular frequency, ω, curves of the materials studied are shown in Fig. 1 at a reference temperature of 190°C. A

TABLE II Rheological parameters of the copolymers studied at 190°C and sharkskin characterisation at 160°C

Material	η_0/Pa s	τ_0/s	E_a/kJ mol^{-1}	τ/s
WP0	16000	0.050	22.50	0.0060
WP1	4000	0.015	26.25	0.0031
WP2	4900	0.017	28.33	0.0059
WP3	5700	0.019	31.67	0.0066

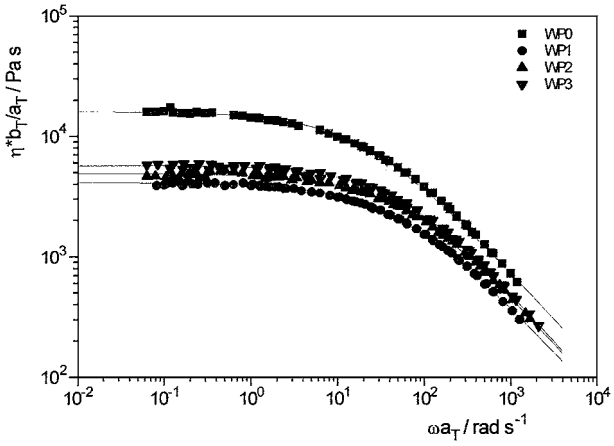

Figure 1 Complex viscosity *versus* reduced angular frequency at 190°C for all the metallocene-catalysed PE's studied: (■) WP0, (●) WP1, (▲) WP2 and (▼) WP3.

characteristic Newtonian behaviour is clearly exhibited by all the studied samples, being more pronounced in the case of the copolymers that consequently show lower values of M_w, Newtonian viscosities, η_0, relaxation time, τ_0, and flow activation energy, E_a. The results are listed in Table II. The methods used to estimate these rheological parameters are described elsewhere [27]. The values obtained are those typical of linear polymers. The slight increase in the value of E_a for the copolymers is most probably due to the presence of butyl branches [27].

3.2. Capillary extrusion

3.2.1. The distortion regimes

Flow curves of the various materials studied are shown in Fig. 2 at 160°C. The sharkskin regime, characterised by a periodic distortion along the extrudate surface, is observed in all cases providing that a critical value of shear stress of about $\sigma_{c1} = 0.16$ MPa is reached. This value, which has been reported to be independent of temperature, M_w and SCB content, is well inside the limiting values found in the literature for linear PE [12, 18, 29] that in general range between 0.1 and 0.2 MPa. A second distortion regime at a shear stress of about $\sigma_{c2} = 0.32$ MPa for the homopolymer and 0.36 MPa for the copolymers has also been observed. The difference observed between homo and copolymers can be associated entirely to differences in M_w [18]. At this critical value, the slip-stick transition characterised by sudden oscillations in the extrusion pressure and the appearance of alternatively smooth and rough or "bamboo-like" extrudates takes place. In this case it is assumed that beyond the critical shear stress, σ_{c2}, a large slip of the material along the die wall does occur. It has been suggested that this macroscopic slip could be originated from an alteration of the nature of the interfacial hydrodynamic boundary condition near the wall along the capillary die. A disentanglement coil-stretch transition has been proposed as the main cause of this transition. This recent theory for melt/solid interfacial slip developed by Brochard and de Gennes [16] establishes that the stress σ_{c2} shared by a number of ν chains per unit area at the wall can be given by:

$$\sigma_{c2} = \nu \kappa_B T / N_e^{0.5} a \qquad (1)$$

$T(K)$ being the temperature, N_e the number of polymer segments between adjacent entanglements and a the Rouse length. The dependence found between the magnitude of the slip, given by a distance along the die b, and the critical shear stress σ_{c2}, with the molecular weight ($b \sim M_w^{3.5}$; $\sigma_{c2} \sim M_w^{-0.5}$) may reveal the molecular origin of the phenomenon [18].

The flow curves performed at 145, 160 and 190°C for the homopolymer (WP0) are shown in Fig. 3. It can be observed an increase of the critical stress for the onset of the slip-stick transition, σ_{c2}, with temperature. As can be seen in Fig. 4, the quantity σ_{c2}/T is lower at low temperature in agreement with previous results obtained for High Density Polyethylenes (HDPEs) [30]. The theory of Brochard and de Gennes also postulates

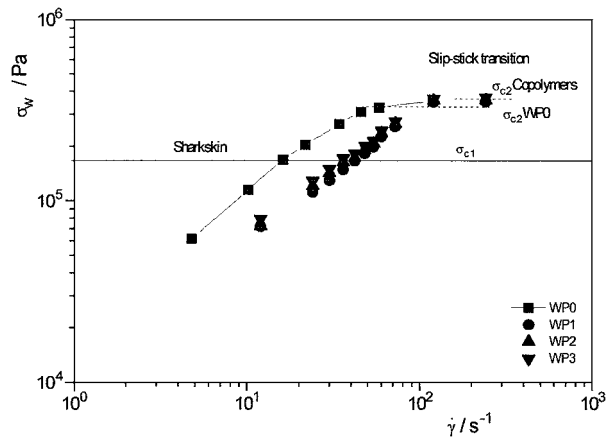

Figure 2 Uncorrected flow curves of shear stress *versus* shear rate at 160°C for the polymers studied. The symbols are as in Fig. 1. Dashed lines represent the critical values of the shear stress for the onset of the distortion regimes.

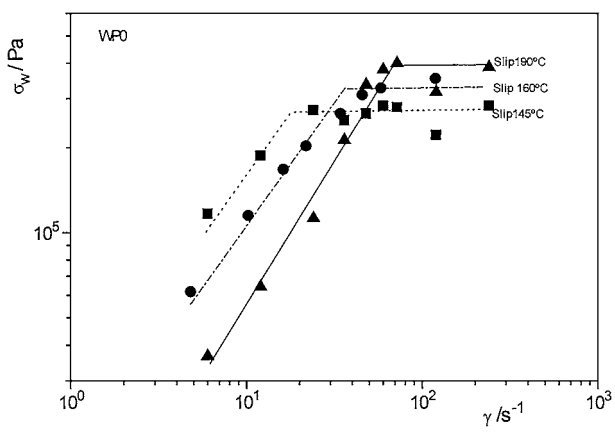

Figure 3 Flow curves for WP0 at different temperatures. (■) 145°C, (●) 160°C, and (▲) 190°C . Lines are drawn only for the sake of clarity.

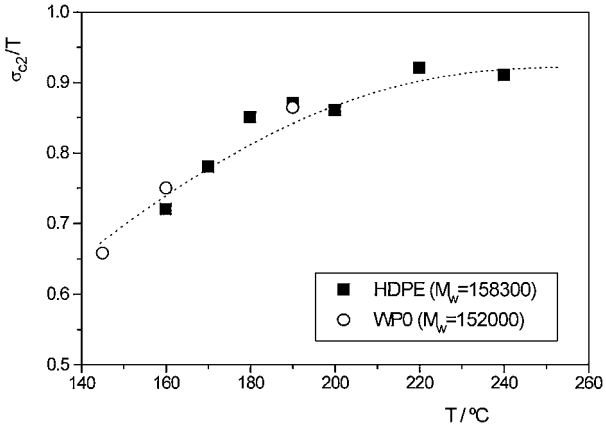

Figure 4 Temperature-dependence of the critical stress, σ_{c2}. (○) WP1, and (■) literature results of a HDPE of $M_w = 158000$ [18]. In order to compare our results with previous literature data [30], the magnitude of the temperature that normalizes the critical stress in the y-axis has been set to Kelvin.

that the critical shear stress for the observed slip scales linearly with temperature. It is reasonable to assume that the molecules near the wall are attached through several sites along their backbone. The molecules in the bulk are connected to those points through entanglements. Under flow the molecules are stretched, and when a critical stress is reached the chains can be detached from the interface, resulting in a boundary slip condition. In a similar way to our results, Wang and Drda [30] have found that σ_{c2}/T increases with temperature up to a constant value at around 200°C. Following Wang *et al*. the effect can be explained by the formation of a temperature dependent flow induced ordered phase that reduces the effective entanglement density at the wall.

In the case of sharkskin regime the situation becomes much more puzzling and there is not a clear explanation for this phenomenon. In a similar way to the slip-stick transition, the existence of the critical shear stress for the sharkskin regime σ_{c1}, has been theoretically approached in the "Interfacial Molecular Instability" (IMI) model developed by Wang *et al*. [17, 18]. These authors have considered this stress as the critical value for a coil-stretch transition of the layer formed by interfacial chains localized at the exist of the die. However, the characteristic periodicity of sharkskin has been assigned not only to the cohesive failure involving disentanglement among bulk chains located away from the die wall near the exit but also to some degree of localized slip.

Morphological details of the cooled extrudates obtained in the sharkskin region, like those shown in Fig. 5, have been analysed for the materials studied. All the extrudates have been collected at 160°C under similar values of shear stress, 0.31–0.35 MPa, just before the slip-stick transition. It can be observed that the sharkskin distortion is a perfect periodic helix. This distortion is characterised by a periodicity, τ, defined by the ratio λ/V, being λ the wavelength between neighbouring ridges and V the linear velocity of the extrudate. The values of periodicity have been calculated (see Table II) following the procedure described by Wang *et al*. [17, 18]. The sharkskin periodicity can be defined

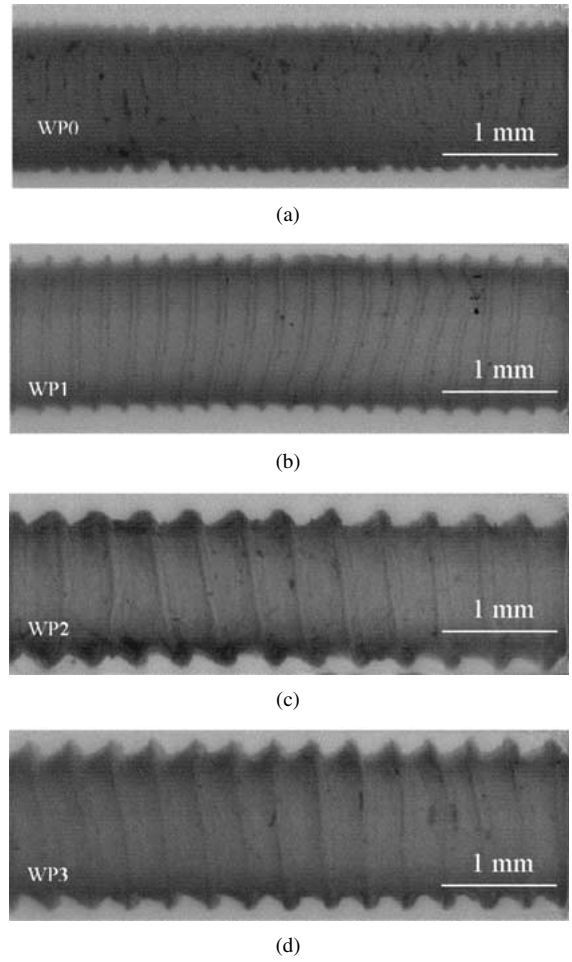

Figure 5 Micrographs of polymer extrudates taken at $T = 160$°C and $\sigma = 0.31$–0.33 MPa below the slip-stick transition, (a) WP0, (b) WP1, (c) WP2 and (d) WP3.

as a function of the sharkskin wavelength between neighbouring ridges, λ, the die swell ratio, D'/D, and the shear rate, $\dot{\gamma}$:

$$\tau = \frac{8\lambda}{D\left(\frac{D}{D'}\right)^2 \dot{\gamma}} \tag{2}$$

The results have been compared with that obtained in similar conditions of stress and temperature in a series of *m*PE-s [31] and they are of the same order of magnitude. Furthermore there exists a linear correlation between τ and η which suggests a direct connection between distortion dynamics and bulk stress relaxation involving overall molecular dynamics [17, 18, 29]. This is in disagreement with Rutgers and Mackley results that are concurrent with a faster chain dynamics involved in the recoil of stretched chains at the exit [11]. These latter authors still support the Cogswell picture [6] that sharkskin defects are due to a real rupture of extrudate surface as a consequence of the acceleration and surface stress concentration at the die exit. In fact, they have recently claimed a direct correlation between surface instabilities and surface stress concentration at the exit as well as with the melt strength of the polymers. In the same way, the studies by El Kissi *et al*. [10] lead to the conclusion that sharkskin is a die exit phenomenon due to the relaxation of stretch strains, with slip having a minor effect on its appearance.

The subject is still very complex and at this stage it is beyond the aim of this paper to further discuss the origin of this important feature of polymer melts. Alternatively we will focus our study in another interesting phenomenon: the elimination of distortion regimes at low temperatures.

3.2.2. The temperature window

In Fig. 6 the pressure exerted on the piston is represented against temperature for two different piston speeds for sample WP0. At speed of 2 mm/min the flow is steady during the whole test at any temperature. On increasing temperature one can observe that the extrudates become smooth and the typical "cracks" of sharkskin distortion only appear when one reaches a temperature of 148.5°C. On the other hand at higher piston speed (4 mm/min) the characteristic pressure oscillations of the slip-stick transition can be easily detected. However, the extrudate comes out throught the orifice differently from the typical "bamboo-like" distortion of this regime although the pressure oscillations are somewhat transferred to the surface of the extrudates. The typical "cracks" in the "stick" portion of the "bamboo-like" extrudate only appear clearly at 147.5°C. To resume the results one can conclude that below a certain temperature the characteristic irregularities of the extrudates are totally absent and they rather appear as smooth-like type. It is worthwhile to mention that all the effects occur at pressures within the normal limits of shark-skin and slip-stick transitions. The temperature flow behaviour above described is exhibited by all the studied samples although a correction in piston speed has to be applied to compensate for M_w effect.

To further illustrate this important feature we have depicted in Figs 7 and 8 the various stages of the extrudates as they evolve with temperature at a piston speed of 10 mm/min. Below 140°C the extrudate is perfectly smooth (see top picture in Fig. 7) though the stres level is very high (Fig. 8). We are within the temperature window. As the temperature is increased the first distortion appears. The second picture clearly reveals the bamboo-like structure characteristic of the slip-stick transition.

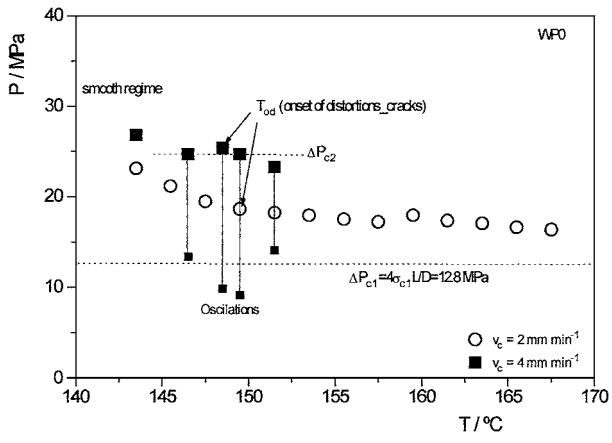

Figure 6 Pressure vs. temperature traces for polymer WP0 at 0.5°C /min at ram speed of 2 and 4 mm/min. The lines indicate the oscillation in the values of the measured pressure values for the slip-stick transition. The arrows show the temperature at which the distortion appears.

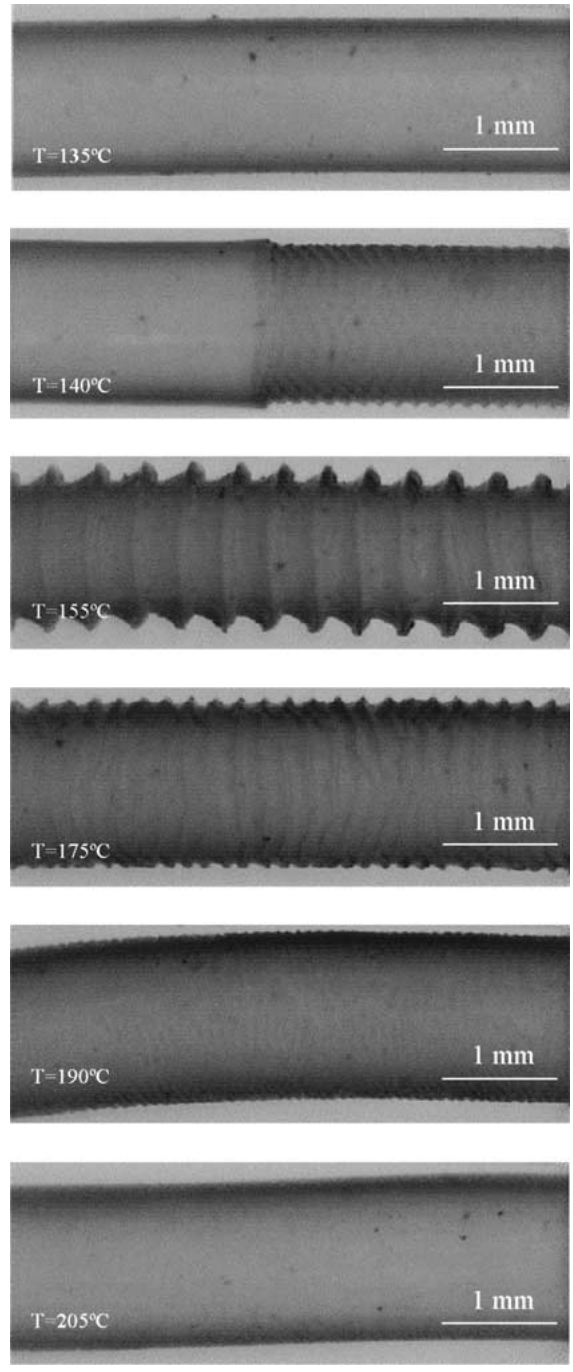

Figure 7 Micrographs of extrudates of the copolymer WP3 at indicated T and piston velocity 10 mm min^{-1}.

If one further increases the temperature one reaches the shark-skin region. The evolution of the periodic structure with temperature can be followed in pictures 3 to 5 of Fig. 7. All the effects are concurrent with a shear stress decrease. The bottom picture illustrates the smooth structure once the stress comes down below σ_{c1}.

Temperature values for the onset of the distortion regime, T_{od}, are collected in Table III. A systematic decrease on T_{od} with the SCB content can be depicted from Fig. 9. The results obtained for the homopolymer and the copolymer with the lowest content in SCB (WP1) nicely coincide with the temperature window of minimum resistance to flow obtained by Keller and co-workers [21–26] for polydisperse high density polyethylenes (HDPE) with varying M_w from 200 K to 900 K. However a notable difference for the high SCB

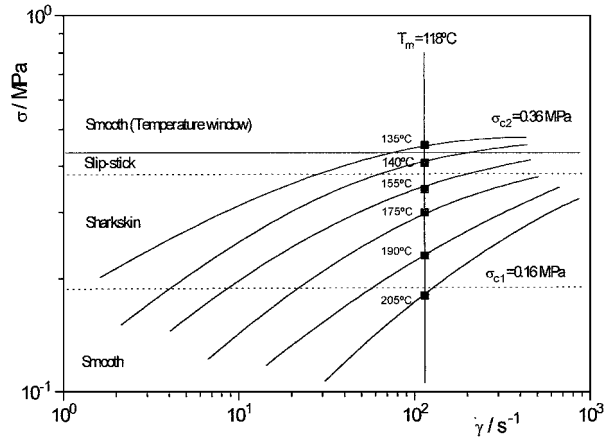

Figure 8 Schematic representation of the temperature sweep for the material WP3. Symbols in the figure correspond to the level of shear stress measured during the extrusion of extrudates in Fig. 8.

content polymers is clearly visible (WP2 and WP3). The decrease in T_{od} of about 5°C for the copolymer with 6 SCB/1000 C (WP2) and of about 10°C for the copolymer with 11 SCB/1000 C (WP3) is particularly striking. This behaviour is reminiscent of that observed by Waddon and Keller in a material with 4.9 branches per thousand carbons but with higher M_w and polydispersity index [22]. The results obtained by these authors material are also included in Fig. 9.

As can be seen in Fig. 9, the dependence of T_{od} with SCB content parallels the tendency followed by the melting temperature, T_m. This result suggests that the stability zone, i.e., the stable extrusion temperature window, may be related to T_m. Following the idea of Keller and co-workers [21–26] the cause of the disappearance of instabilities in the extrudates could be the formation of a mobile hexagonal phase arising through the flow-induced alignment of presumably adsorbed chains at the capillary wall. The decrease of the temperature window with the presence of branches was then interpreted as the side group raising the new mesophase (crystal) free energy and the resulting decrease in the temperature at which a transition to the hexagonal phase should occur. The elimination of the distortions within the temperature window has been explained both by the molecular disentanglement/slip and by the melt cracking mechanisms supporters. Wang *et al.* [18] has suggested that in such an ordered phase, adsorbed chains may remain disentangled and may not return to an entangled state, so the molecular mechanism causing distortions would be no longer present. On the other hand, Cogswell [9] suggested that the flow-induced molecular ordering would increase the melt cohesiveness and thus the melt strength of the fluid polymer.

TABLE III Temperature for the appearance of the distortions (°C)

v_p/mm min^{-1}	WP0	WP1	WP2	WP3
2	148.5	–	–	–
4	147.5	–	148.5	140.0
10	–	148.5	146.5	140.5
10 (treated)[a]	–	146.5	144.5	136.5

[a]Melted at 160°C during 15 minutes and then cooled to $T_m + 10$ before proceeding with the extrusion experiment.

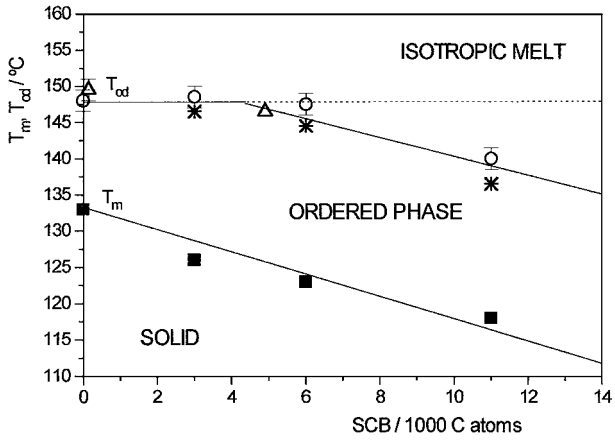

Figure 9 Short chain branching content dependence of the temperature for the onset of distortion regimes and melting temperature. (○) Our materials, (∗) Our treated materials (see text), (△) Literature HDPE data [21–26], and (■) T_m of *m*-PEs.

The location of T_{od} and its relation with T_m allows one to define two zones depending on the temperature state: one zone located between T_m and T_{od} where an ordered phase may coexist with the pure melt and a second zone over T_{od}, where the melt would be purely isotropic. We must emphasise that in the case of copolymers T_{od} is nearly $T_m + 23$. A somewhat lower value of T_{od} has been obtained for the homopolymer ($T_m + 15$). This finding suggests that the temperature of around 150°C may be a thermodynamic upper limit over which the mesophase is no longer stable.

A minimum shear stress value along the temperature sweeps around T_{od} has not been found in any case. However, Keller and co-workers [21–26] observed a critical value in the piston speed and a low-end cut-off in the M_w, over which a decrease in the pressure level occurred. That is, for a given piston velocity, the M_w has to exceed a certain critical value for the effect to set in. They located this critical M_w in the range between 220.000 and 400.000, far above the values of the materials studied here. We would like to emphasize that although no minimum flow resistance has been observed in our materials, the extrudate distortions never appear in the temperature range between $T_m + 10$ and T_{od}.

Finally, the measurements carried out with samples free of crystallisation memory (see experimental section) have given similar results. These measurements have been performed only with the copolymers and at the piston speed of 10 mm/min. As can be seen in Fig. 9, the temperatures for the onset of the distortions have been found to decrease around 2–4°C (see Table III), so, when the crystallisation memory is not removed a more stable mesophase probably develops.

4. Conclusions

We have carried out an investigation at different temperatures into the basic physical aspects that govern capillary flow phenomena in polyethylenes obtained by metallocene catalysts systems. The results of this research reveal a common behaviour in all the samples studied: the clear appearance of distortion regimes

when certain critical values of shear stress are reached. There seems to exist a correlation between distortion and molecular dynamics, but the issue is still highly controversial and our study cannot support plainly any of the existing models. However, as a clear result, a low temperature window for the smooth extrusion has been located in all the materials. The window covers a broad temperature range of temperatures extending up to 23°C above the melting point. Within this window the material can be nicely extruded free of any distortion. This temperature window seems to be related with SCB in a similar way to the melting temperature, T_m, so the possibility of the existence of an ordered mesophase ought to be considered. For the homopolymer, a similar value of $T_{od} = 148$°C but with a narrower temperature window (up to $T_m + 15$) than for the copolymer with the lowest SCB content has been observed. This result suggests a thermodynamic upper temperature limit at around 150°C for the existence of this mesophase. An accompanying minimum flow resistance value, previously detected by other studies cannot be observed in our samples. The most probable explanation is the low M_w that characterises the materials studied here. The above findings are of great relevance for polymer applications taking into account the actual processing limitations of linear metallocene catalysed polyethylenes of narrow molecular weight distribution in conventional operations such as extrusion and blow moulding.

Acknowledgements

Thanks are due to the CICYT (Grant MAT-99-1053) for the support of this investigation. The authors also acknowledge Repsol-YPF for the permission to publish these data.

References

1. Y. HONG, J. J. COOPER-WHITE, M. E. MACKAY, C. J. HAWKER, E. MALMSTRÖM and N. REHNBERG, *J. Rheol.* **43** (1999) 781.
2. E. E. ROSENBAUM, S. K. RANDA, S. G. HATZIKIRIAKOS, C. W. STEWART, D. L. HENRY and M. BUCKMASTER, *Polym. Eng. Sci.* **40** (2000) 179.
3. A. V. RAMAMURTHY, *J. Rheol.* **30** (1986) 337.
4. R. H. MOYNIHAN, D. G. BAIRD and R. RAMANATHAN, *J. Non-Newt. Fluid Mech.* **36** (1990) 255.
5. J.-M. PIAU, S. NIGENAND and N. EL KISSI, *ibid.* **91** (2000) 37.
6. F. N. COGSWELL, J. R. BARONE, N. PLUCKTAVEESAK and S. Q. WANG, *J. Rheol.* **43** (1999) 245.
7. E. R. HOWELLS and J. J. BENBOW, *Trans. J. Plast. Int.* **30** (1962) 240.
8. O. BARTOS and J. HOLOMEK, *Polym. Eng. Sci.* **11** (1971) 324.
9. F. N. COGSWELL, *J. Non-Newt. Fluid Mech.* **2** (1977) 37.
10. N. EL KISSI, J.-M. PIAU and F. TOUSSAINT, *ibid.* **68** (1997) 271.
11. R. RUTGERS and M. MACKLEY, *J. Rheol.* **44** (2000) 1319.
12. D. S. KALIKA and M. M. DENN, *ibid.* **31** (1987) 815.
13. S. G. HATZIKIRIAKOS and J. M. DEALY, *ibid.* **36** (1992) 703.
14. W. B. BLACK and M. D. GRAHAM, *Phys. Rev. Lett.* **77** (1996) 956.
15. D. A. HILL, *J. Rheol.* **42** (1998) 581.
16. F. BROCHARD and P. G. DE GENNES, *Langmuir* **8** (1992) 3033.
17. S. Q. WANG and P. A. DRDA, *J. Rheol.* **40** (1996) 875.
18. *Idem.*, *Macromol. Chem. Phys.* **198** (1997) 673.
19. Y. M. JOSHI, A. K. LELE and R. A. MASHELKAR, *J. Non-Newt. Fluid Mech.* **94** (2000) 135.
20. A. L. YARIN and M. D. GRAHAM, *J. Rheol.* **42** (1998) 1491.
21. A. J. WADDON and A. KELLER, *J. Polym. Sci.:Part B: Polym. Phys.* **28** (1990) 1063.
22. *Idem.*, *ibid.* **30** (1992) 923.
23. J. W. H. KOLNAAR and A. KELLER, *Polymer* **35** (1994) 3863.
24. *Idem.*, *ibid.* **36** (1995) 821.
25. *Idem.*, *ibid.* **38** (1997) 1817.
26. *Idem.*, *J. Non-Newt. Fluid Mech.* **69** (1997) 71.
27. J. F. VEGA, A. SANTAMARÍA, A. MUÑOZ-ESCALONA and P. LAFUENTE, *Macromolecules* **31** (1998) 3639.
28. J. MARTÍNEZ-SALAZAR, M. SÁNCHEZ CUESTA and F. J. BALTÁ CALLEJA, *Colloid and Polym. Sci.* **265** (1987) 239.
29. J. F. VEGA, M. FERNÁNDEZ, A. SANTAMARÍA, A. MUÑOZ-ESCALONA and P. LAFUENTE, *Macromol. Chem. Phys.* **200** (1999) 2257.
30. S. Q. WANG and P. A. DRDA, *Macromolecules* **29** (1996) 4115.
31. C. DEEPRASERTKUL, C. ROSENBLATT and S. Q. WANG, *Macromol Chem. Phys.* **199** (1998) 2113.

Received 19 September 2001
and accepted 21 February 2002